Distinct molecular mechanisms and divergent endocytotic pathways of AMPA receptor internalization

Jerry W. Lin[1,2], William Ju[3,4], Kelly Foster[1,2], Sang Hyoung Lee[1,2], Gholamreza Ahmadian[3,4], Michael Wyszynski[1,2], Yu Tian Wang[3,4] and Morgan Sheng[1,2]

[1] *Howard Hughes Medical Institute, Massachusetts General Hospital (Wellman 423), 50 Blossom Street, Boston, Massachusetts 02114, USA*

[2] *Department of Neurobiology, Harvard Medical School, 220 Longwood Ave., Boston, Massachusetts 02115, USA*

[3] *Programme in Brain and Behavior and Division of Pathology, Hospital for Sick Children, 555 University Ave., Toronto, Ontario M5G 1X8, Canada*

[4] *Department of Laboratory Medicine and Pathobiology, University of Toronto, 100 College St., Toronto, Ontario M5G 1X8, Canada*

Internalization of postsynaptic AMPA receptors depresses excitatory transmission, but the underlying dynamics and mechanisms of this process are unclear. Using immunofluorescence and surface biotinylation, we characterized and quantified basal and regulated AMPA receptor endocytosis in cultured hippocampal neurons, in response to synaptic activity, AMPA and insulin. AMPA-induced AMPA receptor internalization is mediated in part by secondary activation of voltage-dependent calcium channels, and in part by ligand binding independent of receptor activation. Although both require dynamin, insulin- and AMPA-induced AMPA receptor internalization are differentially dependent on protein phosphatases and sequence determinants within the cytoplasmic tails of GluR1 and GluR2 subunits. AMPA receptors internalized in response to AMPA stimulation enter a recycling endosome system, whereas those internalized in response to insulin diverge into a distinct compartment. Thus, the molecular mechanisms and intracellular sorting of AMPA receptors are diverse, and depend on the internalizing stimulus.

The AMPA class of ionotropic glutamate receptors mediates most of the fast excitatory synaptic transmission in mammalian brain[1]. Changing the responsiveness of postsynaptic AMPA receptors offers a powerful way to regulate excitatory synaptic transmission. Among the mechanisms proposed for modification of AMPA receptor activity, one of the simplest is a change in the number of AMPA receptors in the postsynaptic membrane. Studies suggest that AMPA receptors can move in and out of the postsynaptic membrane on a rapid time scale (for review, see ref. 2). Moreover, changes in postsynaptic membrane trafficking or in synaptic targeting of AMPA receptors have been correlated with alterations in synaptic efficacy[2–9].

In developing neurons in culture, synaptic expression of AMPA receptors is modulated over a period of days by relative levels of AMPA and NMDA receptor activity[10–12]. Mature neurons in culture also exhibit slow changes in synaptic AMPA receptor expression in response to chronic changes in endogenous activity[9,13,14]. On a faster time scale, induction of long-term depression (LTD) or acute application of AMPA or insulin can induce a loss of AMPA receptors from the cell surface of cultured hippocampal neurons within minutes[3,6,9,15]. Conversely, induction of long-term potentiation (LTP) and activation of CaMKII are correlated with a rapid recruitment of AMPA receptors to the postsynaptic membrane[5,8]. Thus, the synaptic content of AMPA receptors can change bidirectionally on a fast time scale and result in altered synaptic transmission.

Little is known about the cell biological pathways or molecular mechanisms of postsynaptic AMPA receptor trafficking. To date, studies of AMPA receptor trafficking have focused on the presence or absence of AMPA receptors at synaptic sites, or on internal versus surface expression[3–10,15–18]. However, the multiple subunits of AMPA receptors interact differentially with diverse cytoplasmic proteins including GRIP/ABP, PICK1, NSF and SAP97, all of which have been implicated in synaptic targeting of AMPA receptors[3,5,17,19–27]. The diversity of AMPA receptor protein interactions, and their regulation by phosphorylation[28], suggest that AMPA receptor trafficking is likely to be regulated by varied mechanisms.

Here we report that multiple distinct pathways exist for AMPA receptor endocytosis in cultured hippocampal neurons. We have quantified a basal rate of AMPA receptor internalization, which can be enhanced by a variety of stimuli including synaptic activity, ligand binding to AMPA receptors, insulin and calcium influx. Different internalizing stimuli use distinct intracellular signaling mechanisms, different endosomal sorting pathways and distinct sequence determinants within AMPA receptor subunits to effect AMPA receptor endocytosis.

Results

Ligand-dependent endocytosis of AMPA receptors

Translocation of AMPA receptors from cell surface to intracellular compartments was visualized and quantified by an 'antibody feeding' immunofluorescence internalization assay in hippocampal neurons cultured at medium density (15–18 days *in vitro*; see Methods)[3]. In control conditions, a small but significant degree of basal AMPA receptor internalization was detectable by 10 minutes (**Fig. 1a**). Treat-

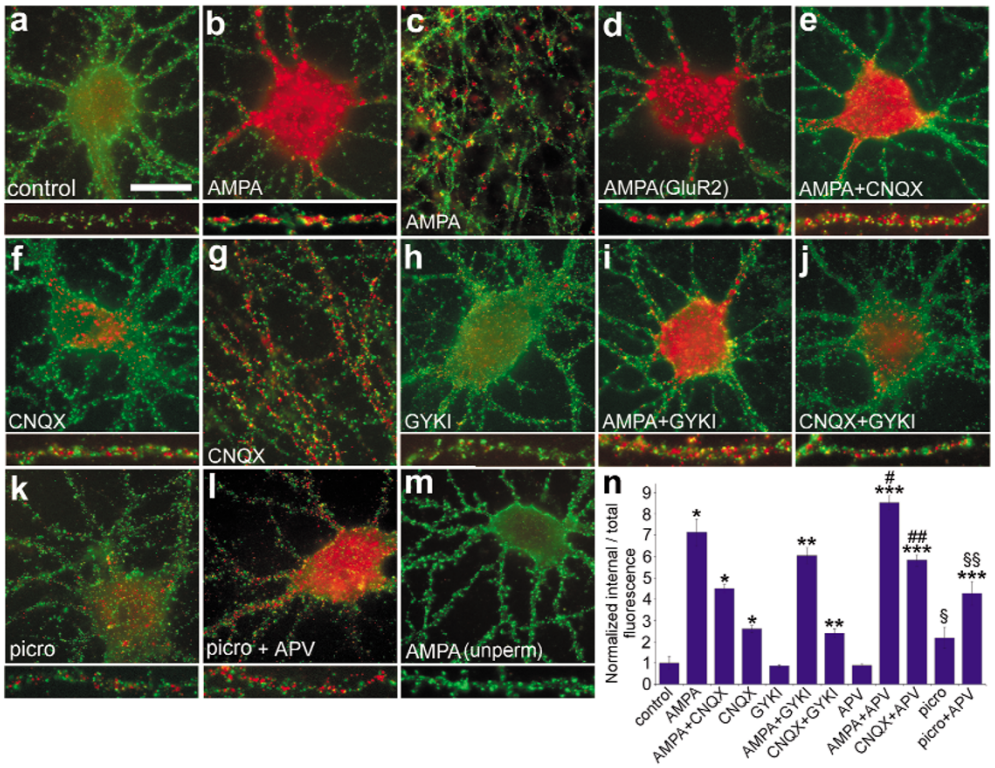

Fig. 1. Rapid ligand-dependent endocytosis of AMPA receptors in cultured hippocampal neurons. Endocytosis of AMPA receptors (GluR1, unless otherwise stated) was visualized and quantified by the immunofluorescence internalization assay after 10-min exposure to various drugs, as indicated. Pre-labeled AMPA receptors remaining on the surface are in green, internalized receptors in red (see Methods). (**a**) Basal AMPA receptor internalization at 10 min. (**b**, **c**) Stimulation of AMPA receptor internalization by AMPA (100 μM) in neuronal cell bodies (**b**) and in distal dendrites (**c** and inset of **b**). (**d**) GluR2 internalization stimulated by AMPA (100 μM). (**e**) AMPA + CNQX (30 μM). (**f**, **g**) CNQX (30 μM). (**h**) GYKI 52466 (30 μM). (**i**) AMPA + GYKI 52466. (**j**) CNQX and GYKI 52466. (**k**) Picrotoxin (100 μM). (**l**) Picrotoxin + APV (100 μM). Upper part of each panel (except **c** and **g**), typical pattern of internalized AMPA receptors in the cell body and proximal dendrites. Lower inset, staining pattern of internalized receptors in more distal dendrites. (**m**) AMPA-treated cells stained according to the immunofluorescence internalization assay, but omitting the methanol permeabilization step. (**n**) Quantitation of AMPA receptor internalization, measured as the ratio of internalized (red) / total (red + green) fluorescence, normalized to 10 min control. Histograms show mean ± s.e.m. Conditions quantified include those illustrated in (**a–l**) as well as 100 μM APV, 100 μM APV + 100 μM AMPA, 100 μM APV + 30 μM CNQX. Control, vehicle-treated culture. * $p < 0.001$ compared with control; ** $p < 0.001$ compared with GYKI and $p < 0.001$ compared with control; *** $p < 0.001$ compared with APV and $p < 0.001$ compared with control; # $p < 0.01$ compared with AMPA; ## $p < 0.001$ compared with CNQX;/ $p < 0.05$ compared with control;/ /$p < 0.01$ compared with control, $p < 0.01$ compared with APV, and $p < 0.01$ compared with picrotoxin. Scale bar, 20 μm for large panels, 6.6 μm for insets.

ment with AMPA (100 μM) greatly enhanced internalization of AMPA receptor subunit GluR1 (**Fig. 1b**, **c** and **n**), consistent with previous results[15]. The internalized AMPA receptors accumulated in bright red puncta of variable size and shape, in both the cell body and dendrite shafts of neurons (**Figs. 1b**, inset, and **c**). Similar results were obtained using an antibody against the extracellular region of GluR2 (**Fig. 1d**). An antibody directed against an intracellular epitope of GluR2/3 produced no staining in this protocol (data not shown), excluding the possibilities that AMPA might induce a non-specific uptake of antibodies, or that the plasma membrane of live neurons is permeable to antibodies. Furthermore, elimination of the permeabilization step during staining abolished red labeling (**Fig. 1m**), indicating that the neuronal plasma membrane remained intact after fixation, and verifying that the Cy3 signal represented internalized AMPA receptors.

AMPA receptor internalization stimulated by AMPA was only partially inhibited (~35%) by the competitive antagonist CNQX (30 μM, **Fig. 1e** and **n**). Remarkably, 10 minutes of treatment with CNQX alone induced internalization of AMPA receptors in both neuronal soma and dendrites (**Fig. 1f**, **g** and **n**). This finding suggested that a ligand-induced conformational change in the receptor was enough to stimulate AMPA receptor endocytosis, independent of receptor activation. GYKI 52466 (30 μM), a non-competitive antagonist of AMPA receptors, did not stimulate endocytosis of AMPA receptors (**Fig. 1h** and **n**). Moreover, GYKI 52466 had only a minor inhibitory effect on AMPA-induced internalization of AMPA receptors, and no effect on CNQX-induced endocytosis (**Fig. 1i**, **j** and **n**). APV (100 μM), a blocker of NMDA receptors, did not inhibit either AMPA- or CNQX-induced endocytosis of AMPA receptors (**Fig. 1n**). On the contrary, APV significantly potentiated the AMPA and CNQX effects (**Fig. 1n**).

The partial inhibition of AMPA-stimulated AMPA receptor internalization by CNQX (**Fig. 1n**) suggested that some of the AMPA-induced endocytosis was due to AMPA receptor activation. Consistent with this, AMPA-induced endocytosis of AMPA receptors was also reduced (~50%) by nimodipine (5 μM; **Fig. 5m**), an L-type voltage-gated calcium channel blocker, and by extracellular EGTA (10 mM, data not shown), both of which would prevent depolarization-mediated calcium influx in response to AMPA stimulation. Importantly, CNQX-induced AMPA receptor internalization was unaffected by nimodipine (**Fig. 5m**). Taken together, these data indicate that AMPA stimulation of receptor internalization consists of at least two components: one that is due purely to occupancy of the glutamate binding site, and one that is mediated by AMPA receptor activation and subsequent depolarization and calcium influx through voltage-dependent calcium channels.

Picrotoxin, an antagonist of $GABA_A$ receptors, increased AMPA receptor internalization ~2.2-fold over control ($p < 0.05$; **Fig. 1k** and **n**). This picrotoxin effect was not prevented by APV; in fact,

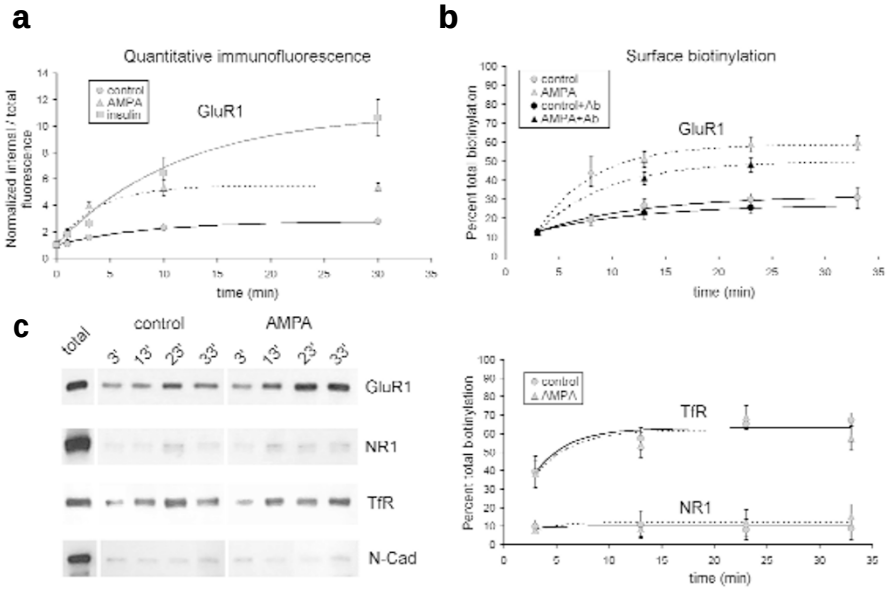

Fig 2. Time course of basal, AMPA-, and insulin-induced internalization of AMPA receptors. (**a**) Time course of AMPA receptor (GluR1) internalization measured by quantitative immunofluorescence (as in **Fig. 1**) in the presence of vehicle alone (control), 100 μM AMPA or 10 μM insulin. (**b**) Time course of basal and AMPA-induced internalization of GluR1 (top) and of transferrin receptor (TfR) and NR1 (bottom), quantified by surface biotinylation assays (white symbols). The time course of GluR1 internalization was also quantified by the surface biotinylation assay after pre-labeling with extracellular GluR1 antibody according to the immunofluorescence internalization assay protocol (+ Ab, black symbols). (**c**) Representative immunoblots of the time course of internalization of GluR1, TfR, NR1 and N-cadherin (N-Cad) by the surface biotinylation assay in control and AMPA-treated cultures. In (**a**) and (**b**), plotted lines represent the best fit to a single exponential curve determined by the least-squares method. Solid line, basal internalization; dotted line, AMPA-induced internalization; gray line, insulin-induced internalization.

APV plus picrotoxin actually enhanced AMPA receptor endocytosis above that caused by picrotoxin alone (~4.3 fold; **Fig. 1l** and **n**). These results indicate that endogenous synaptic activity can stimulate AMPA receptor internalization through an NMDA receptor-independent mechanism.

Time course of AMPA receptor internalization

We measured the time course of AMPA receptor endocytosis under basal and stimulated conditions (**Fig. 2**). In untreated cultures, basal endocytosis of AMPA receptors occurred to a modest extent, as quantified by the immunofluorescence internalization assay,

Fig 3. Continued AMPA receptor internalization during the plateau phase of internalized AMPA receptor signal. (**a–d**) AMPA receptor internalization was measured by the immunofluorescence internalization assay in response to AMPA (**a**, **b**) or insulin (**c**, **d**). In (**a**) and (**c**), surface AMPA receptors were pre-labeled (pre) by applying extracellular GluR1 antibody immediately before AMPA or insulin treatment, as in the standard immunofluorescence internalization assay protocol, and GluR1 internalization was visualized after 10 min of exposure to AMPA or insulin. In (**b**) and (**d**), surface AMPA receptors were post-labeled (post) by applying extracellular GluR1 antibody 20 min after the onset of AMPA or insulin treatment. After post-labeling, endocytosis was allowed to proceed for an additional 10 min. (**e**) Quantitation of the immunofluorescence internalization data shown representatively in (**a–d**). Histograms show mean ± s.e.m. (**f**) AMPA receptor (GluR1) internalization was measured by the surface biotinylation assay using either the standard pre-labeling protocol (pre), in which surface biotinylation was done immediately before treatment with AMPA or insulin, or by the post-labeling protocol, in which surface biotinylation was performed 20 min after the onset of AMPA or insulin treatment. In both cases, the amount of internalization occurring over 10 min was measured. 'Total' lanes, signal from biotinylated cultures that were not surface de-biotinylated with glutathione.

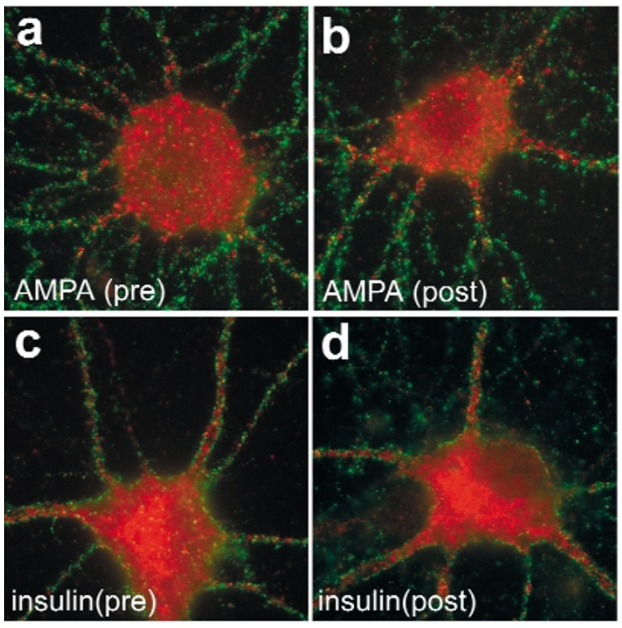

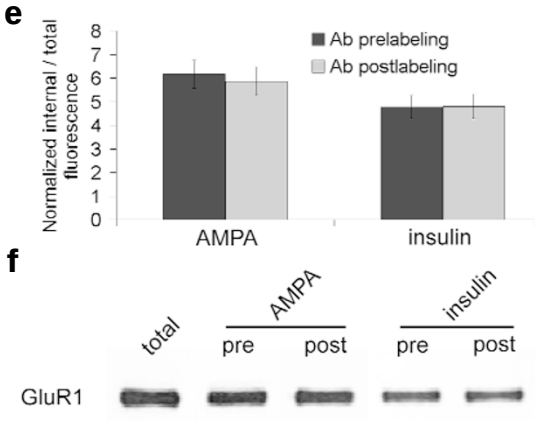

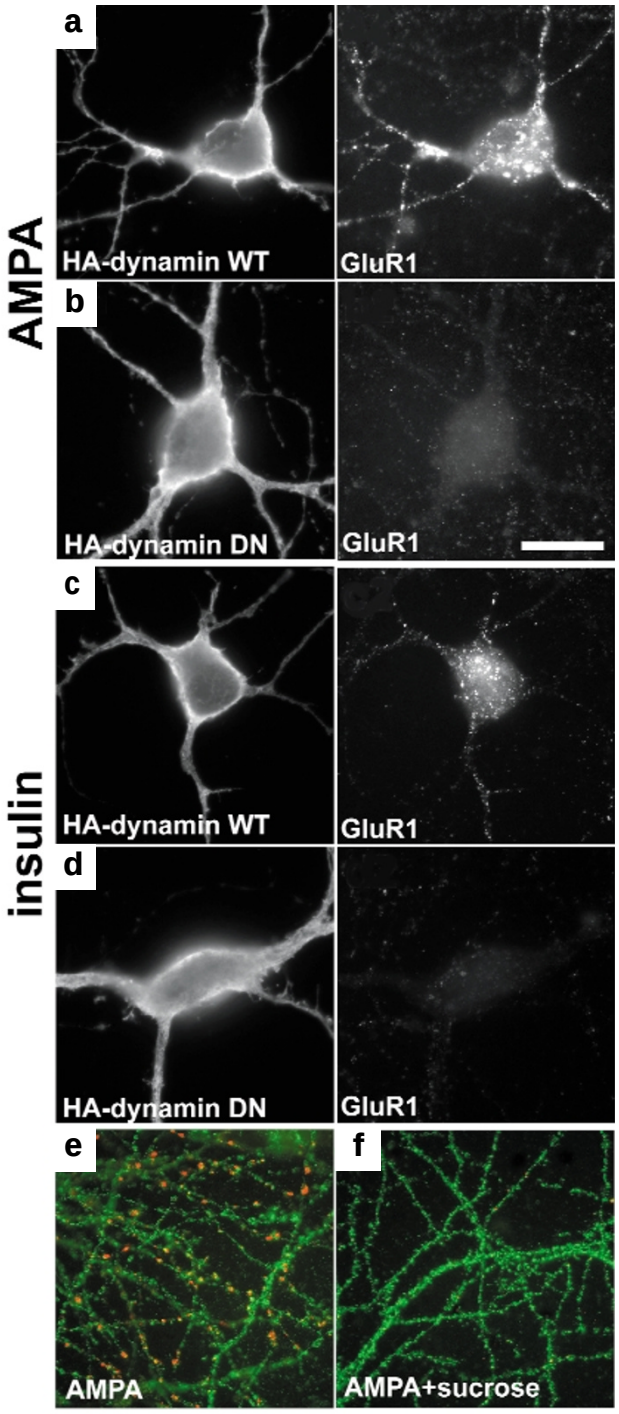

Fig. 4. AMPA- and insulin-induced AMPA receptor internalization through a clathrin-mediated, dynamin-dependent mechanism. Cultured hippocampal neurons were transfected with HA-tagged wild-type dynamin (**a**, **c**) or K44E dynamin dominant negative (DN) mutant (**b**, **d**), and visualized by HA-immunoreactivity and FITC-secondary antibodies. AMPA receptor internalization was stimulated with AMPA (**a**, **b**) or insulin (**c**, **d**), and internalized surface-pre-labeled GluR1 was stained with Cy3 antibodies. Each pair of panels (**a–d**) shows double labeling of the same neuron for dynamin and internalized GluR1. (**e**, **f**) AMPA receptor (GluR1) endocytosis induced by AMPA (**e**) was eliminated by 0.45 M sucrose (**f**). Scale bar, 20 μm.

reaching a plateau after 10–15 minutes (**Fig. 2a**). The rate of internalization, however, was rapid (τ = 7.1 minutes). AMPA enhanced the rate (τ = 3.1 minutes) and degree of AMPA receptor endocytosis, which also reached a plateau by 10–15 minutes (**Fig. 2a**). In contrast, insulin-induced AMPA receptor endocytosis increased over 30 minutes without reaching a plateau (**Fig. 2a**). Because of the different kinetics of the internalization response, insulin had little effect on the time constant of AMPA receptor internalization (τ = 7.6 minutes), compared with control.

We also used surface biotinylation assays to measure AMPA receptor endocytosis (see Methods). Quantified by this independent method, basal internalization of AMPA receptors followed a time course similar to the time course measured by the quantitative immunofluorescence assay (τ = 9.2 minutes, **Fig. 2b**). Similarly, a plateau was reached by ~15 minutes, at which time ~25% of the surface biotinylated AMPA receptors had been internalized. AMPA treatment increased both the rate (τ = 5.2 minutes) and extent of AMPA receptor internalization (~50–60% internalized when plateau was reached at ~15 minutes; **Fig. 2b**). The results from the surface biotinylation method were consistent with the conclusions from the immunofluorescence internalization assays. Moreover, surface biotinylation revealed the specificity of the AMPA effect, because AMPA treatment did not change the rate or extent of internalization of NMDA receptors (NR1 subunit), transferrin receptors (TfR), or N-cadherin (**Fig. 2b**, bottom, and **c**). Internalization of NR1 and N-cadherin was barely detectable in this assay over 30 minutes, in either control or AMPA-stimulated cultures. On the other hand, TfR endocytosis was rapid and robust: ~60% of surface-biotinylated TfR was internalized by 10 minutes in basal conditions, with no change upon AMPA stimulation.

Using the surface biotinylation assay, we also tested the effects of the extracellular GluR1 antibody (applied according to the protocol of the immunofluorescence internalization assay) on the internalization of AMPA receptors. Somewhat surprisingly, we found that the antibody caused an inhibition of surface AMPA receptor endocytosis, both in basal and in AMPA-stimulated conditions (by ~25–30% at all time points examined; **Fig. 2b**). The GluR1 extracellular antibody did not significantly change the time course of basal or AMPA-induced receptor endocytosis or the relative increase in AMPA receptor internalization induced by AMPA treatment. We concluded that although the extracellular GluR1 antibody had a slight inhibitory influence on AMPA receptor internalization, this effect did not alter the validity of relative differences measured by the immunofluorescence internalization assay.

To assess whether AMPA receptor internalization still occurred during the plateau phase of the AMPA receptor internalization response (**Fig. 2a** and **b**), we labeled surface AMPA receptors on live neurons, 20 minutes after onset of AMPA treatment ('post-labeling' protocol; **Fig. 3**). After post-labeling, the amount of AMPA receptor internalization occurring in 10 minutes (**Fig. 3b**) was indistinguishable from that measured when surface AMPA receptors were 'pre-labeled' immediately before AMPA treatment (**Fig. 3a** and **e**). The same results were obtained with pre- and post-labeling of AMPA receptors using surface biotinylation
(**Fig. 3f**). These results implied that in our standard pre-labeling protocol, the plateau of internalized AMPA receptors after 15 minutes reflected a new steady state in which internalization was in equilibrium with recycling to the surface.

We also observed continuing internalization of AMPA receptors with the post-labeling protocol 20 minutes after onset of

treatment with insulin (**Fig. 3d**). The finding that insulin-induced AMPA receptor internalization did not plateau over 30 minutes in the standard immunofluorescence assay is consistent with insulin eliciting a slower rate than AMPA of recycling of internalized AMPA receptors to the cell surface.

Different signaling pathways for endocytosis

Both AMPA- and insulin-induced AMPA receptor internalization depended on the activity of dynamin (**Fig. 4**). Hypertonic sucrose (0.45 M), which disrupts formation of clathrin cages, abolished AMPA-induced AMPA receptor internalization (**Fig. 4e** and **f**), as it does insulin-induced receptor endocytosis[3]. Transfection of neurons with dynamin (K44E), a dominant-negative dynamin mutant, blocked both AMPA- and insulin-induced AMPA receptor internalization (**Fig. 4b** and **d**), whereas wild-type dynamin did not interfere with either form of stimulated AMPA receptor endocytosis (**Fig. 4a** and **c**).

The protein phosphatase calcineurin is implicated in insulin signaling[29,30] and membrane trafficking[31]. Cyclosporin A (0.5 μM), an inhibitor of calcineurin, blocked AMPA receptor internalization induced by insulin (**Fig. 5j** and **m**) but not by AMPA (**Fig. 5f** and **m**), and had no detectable effect on basal internalization (**Fig. 5b** and **m**). FK506 (1 μM) also inhibited insulin-induced AMPA receptor internalization, though the inhibition was less complete than with cyclosporin A (data not shown). Okadaic acid (1 μM), an inhibitor of protein phosphatase-1 (PP1) and protein phosphatase-2A (PP2A), reduced insulin- but not AMPA-induced internalization of AMPA receptors (**Fig. 5g**, **k** and **m**). In fact, okadaic acid enhanced the degree of internalization following AMPA treatment (**Fig. 5m**). Pervanadate (100 μM), a general inhibitor of tyrosine phosphatases, also reduced insulin-dependent AMPA receptor internalization, but had no effect on AMPA-induced internalization (**Fig. 5m**).

As mentioned previously, AMPA-induced AMPA receptor endocytosis was partially blocked by nimodipine (**Fig. 5h** and **m**). Nimodipine, however, had no effect on insulin-induced internalization of AMPA receptors (**Fig. 5l** and **m**). CNQX-induced AMPA receptor endocytosis was unaffected by nimodipine or any inhibitor of insulin-induced internalization (**Fig. 5m**), nor was it potentiated by okadaic acid. These data show that multiple signaling pathways can converge to stimulate AMPA receptor endocytosis.

Differential sorting of internalized AMPA receptors

After endocytosis, internalized proteins can be sorted to various endosomal compartments. Internalized AMPA receptors, after five minutes of treatment with either AMPA or insulin, colocalized extensively in a punctate pattern with early endosomal antigen-1 (EEA1), a marker of early endosomes (**Fig. 6a** and **b**; quantified in **Fig. 6m**). By 15 minutes, however, whereas most of the AMPA-induced internalized AMPA receptors remained colocalized with EEA1 (**Fig. 6c** and **m**), a large fraction (~70%) of insulin-induced internalized AMPA receptors had separated into a membrane compartment that lacked EEA1 (**Fig. 6d** and **m**). Thirty minutes after AMPA stimulation, the majority (~70%) of internalized AMPA receptors were still associated with EEA1-positive compartments, whereas 30 minutes after insulin stimulation, only ~20% of internalized AMPA receptors remained colocalized with EEA1 (**Fig. 6e**, **f** and **m**). Similar subcellular divergence of internalized AMPA receptors was observed when double-label staining was done with TfR (**Fig. 6g** and **h**), which goes through a recycling endosomal pathway, or with syntaxin 13 (**Fig. 6i** and **j**)[32], a SNARE protein localized in tubulovesicular recycling endosomes[33]. Neither AMPA- nor insulin-induced internalized AMPA receptors colocalized with the lysosomal marker LAMP1 even after 30 minutes (**Fig. 6k** and **l**). In unstimulated cultures, the majority of internalized AMPA receptors colocalized with EEA1 at 30 minutes (data not shown).

GluR determinants for AMPA receptor internalization

We 'reconstituted' constitutive and regulated AMPA receptor

Fig. 5. Differential inhibition of AMPA- and insulin-induced AMPA receptor endocytosis by inhibitors of protein phosphatases and L-type calcium channels. (**a–l**) AMPA receptor (GluR1) endocytosis was measured by the immunofluorescence internalization assay at 10 min after treatment with vehicle control, or with various drugs, individually or in combination, as indicated. cycA, 0.5 μM cyclosporin A; oka, 1 μM okadaic acid; nim, 5 μM nimodipine; AMPA, 100 μM AMPA; insulin, 10 μM insulin. (**m**) Quantitation of AMPA receptor (GluR1) internalization at 10 min in response to control (vehicle), AMPA (100 μM), CNQX (30 μM) or insulin (10 μM) treatment, in the presence of various inhibitors: cyclosporin A (0.5 μM), okadaic acid (1 μM), pervanadate (100 μM) or nimodipine (5 μM). * $p < 0.001$ compared with AMPA alone; ** $p < 0.01$ compared with insulin alone. Scale bar, 20 μm.

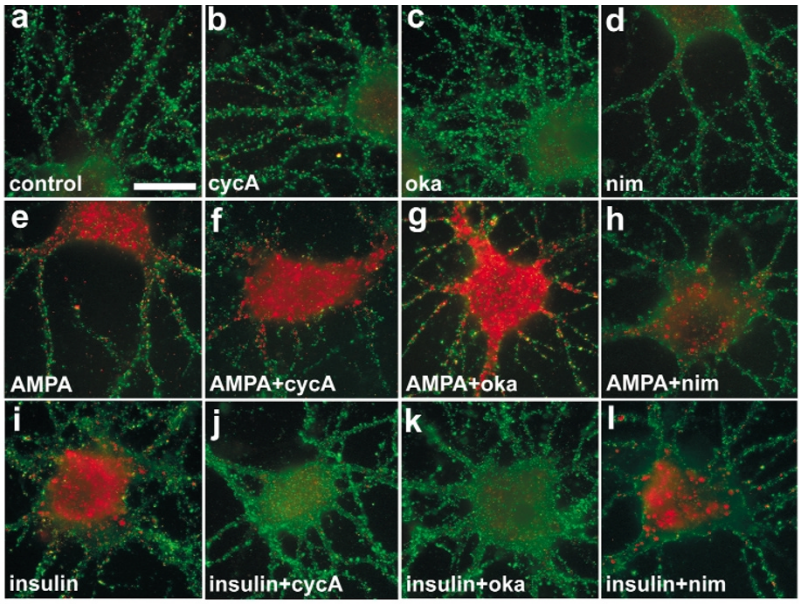

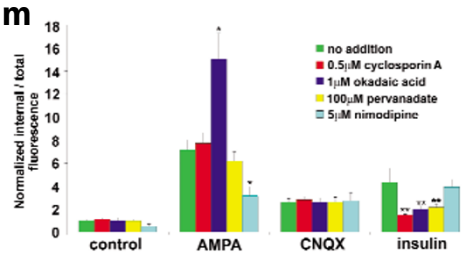

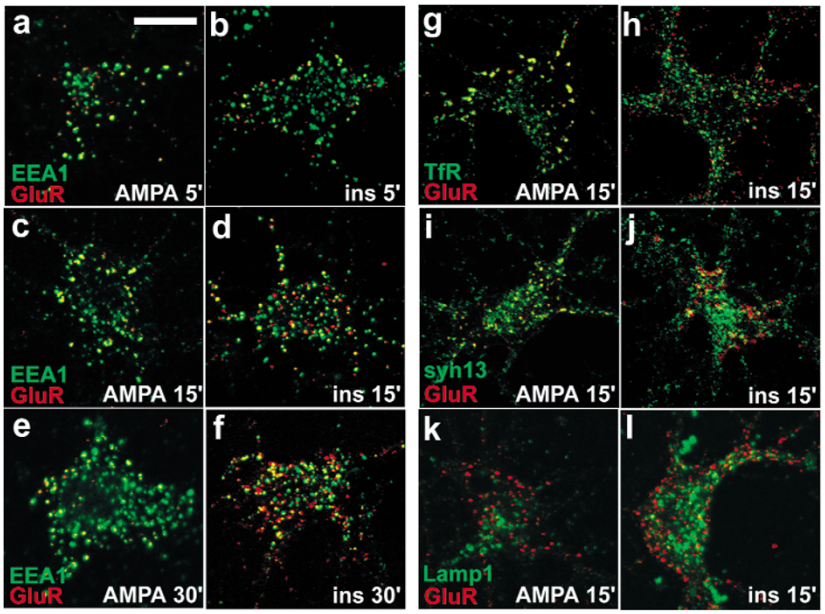

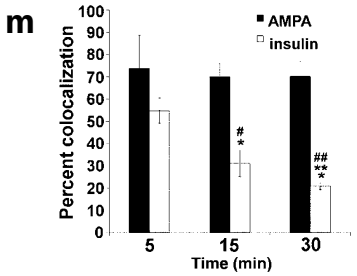

Fig. 6. Differential sorting of internalized AMPA receptors after AMPA and insulin stimulation. (**a–l**) Confocal images showing double-label immunofluorescence for internalized AMPA receptors (red) and EEA1, TfR, syntaxin 13 or Lamp1 (green), at 5, 15 and 30 min after stimulation with AMPA or insulin, as indicated. (**m**) Quantitation of the percentage of internalized GluR1 that colocalized with EEA1 following AMPA or insulin treatment at 5, 15 and 30 min. * $p < 0.001$ compared with insulin at 5 min; ** $p < 0.01$ compared with insulin at 15 min; # $p < 0.001$ compared with AMPA at 15 min; ## $p < 0.001$compared with AMPA at 30 min. Scale bar, 25 μm.

endocytosis in HEK cells expressing N-terminally HA-tagged GluR subunits (see Methods). Thirty minutes after surface labeling, ~25% of surface HA-GluR2 was internalized in basal conditions (**Fig. 7**). Insulin (0.5 μM), AMPA (100 μM), DNQX (30 μM) or CNQX (30 μM) were each able to increase GluR2 endocytosis such that at 30 minutes, ~50% of pre-labeled GluR2 was internalized (**Fig. 7**).

Insulin-induced AMPA receptor internalization requires the C-terminal tail of the GluR2 subunit—insulin has no effect on endocytosis of GluR1 in HEK cells[3]. In contrast, AMPA, DNQX and CNQX stimulated the internalization of both GluR1 and GluR2 homomeric receptors (**Fig. 7**). Deletion of the last four amino acids of GluR2 (Δ880–883), which are important for interaction with PDZ-containing proteins, did not alter the constitutive internalization of GluR2 or its response to insulin, AMPA or DNQX (**Fig. 7**). However, PDZ-containing binding partners of GluR2 such as GRIP and PICK1 are not highly expressed in HEK cells, and therefore this finding does not necessarily exclude their involvement in GluR2 endocytosis. A GluR2 mutant lacking the last 15 amino acids (Δ868–883) was completely unresponsive to insulin, but its internalization was still stimulated by AMPA and DNQX (**Fig. 7**). Conversely, deletion of the membrane-proximal 10 amino acids of the GluR2 tail (Δ834–843) reduced GluR2 internalization in response to AMPA or DNQX, but had little effect on insulin-dependent internalization.

Discussion

AMPA receptor endocytosis: basal, regulated, recycling

A rapid constitutive internalization of AMPA receptors has been inferred from electrophysiological studies[7]. Here we report the visualization of a basal endocytosis of AMPA receptors in cultured neurons and its time course measured by immunofluorescence and surface biotinylation assays. Based on surface biotinylation assays, the kinetics of basal internalization were rapid (τ ~8–9 minutes) and the amount of internalized receptor reached a plateau of ~25% by ~15 minutes. Similarly, the AMPA-stimulated internalization of AMPA receptors showed rapid kinetics and reached a maximum by ~15 minutes. The attainment of the plateau phase could be explained either by completed internalization of a subpopulation of surface AMPA receptors, or by rapid recycling of receptors to the cell surface after internalization. The continued robust internalization of AMPA receptors, measured during the plateau phase following AMPA stimulation (**Fig. 3**), excludes the former possibility and strongly implies the latter.

In contrast to AMPA-stimulated internalization, insulin-stimulated AMPA receptor internalization continued to accumulate over 30 minutes. The simplest explanation for this difference in kinetics is that AMPA receptors that are internalized in response to insulin return more slowly to the surface. This hypothesis is consistent with our finding that AMPA receptors internalized in response to AMPA, but not in response to insulin, remain largely within a recycling endosome system, as defined by colocalization with EEA1, syntaxin 13 and TfR[32–40]. Unlike AMPA, insulin caused a divergence of internalized AMPA receptors out of the pathway delineated by EEA1, syntaxin 13 and TfR into a separate intracellular compartment. This later compartment did not seem to be lysosomal because it did not costain with LAMP1. However, it is possible that internalized AMPA receptors became detached from their antibody by the time they reached degradative organelles.

Taken together, our data suggest that AMPA receptors internalized in response to AMPA treatment quickly reappear on the surface. Insulin, by diverting internalized receptors to a non-recycling pathway, may delay or even prevent the recycling of AMPA receptors back to the surface. Prolonged intracellular sequestration (or degradation) of AMPA receptors may account for the ability of insulin to induce long-lasting depression of synaptic transmission[3]. What is the significance of AMPA receptor cycling in and out of the postsynaptic membrane? A high cycling rate need not alter the steady-state surface expression of AMPA receptors, but it would amplify the effect of inhibition of either endocytosis or exocytosis. Thus, recycling energy is 'wasted' to render synapses more sensitive to stimuli that govern AMPA receptor trafficking in the postsynaptic compartment.

Different modes of AMPA receptor internalization

Several lines of evidence support an activation-independent mechanism of AMPA receptor internalization that depends purely on occupancy of the glutamate binding site. First, CNQX, a competitive antagonist of AMPA/glutamate, by itself induces AMPA receptor internalization in cultured neurons (and this is not prevented by APV or nimodipine). Second, neither AMPA- nor CNQX-induced internalization is blocked by GYKI 52466, a non-competitive antagonist, and GYKI 52466 alone does not stimulate receptor internalization. Third, AMPA and CNQX/DNQX can stimulate internalization of AMPA receptors heterologously expressed in HEK cells. Antagonist-induced internalization of G-protein-coupled receptors has been reported[41]. Here, however, a competitive antagonist acted as a ligand to enhance internalization of an ionotropic glutamate receptor. Presumably, ligand binding induces a conformational change in the AMPA receptor that is 'read' by the cytoplasmic machinery that mediates clathrin- and dynamin-dependent endocytosis. In some contexts, CNQX may indirectly enhance synaptic activity by inhibiting GABAergic neurons[42]. It is therefore possible that CNQX has similar indirect effects on AMPA receptors in hippocampal cultures. However, the reconstitution of AMPA- and DNQX-dependent internalization of AMPA receptors in HEK cells is hard to reconcile with circuitous mechanisms of AMPA receptor endocytosis.

AMPA receptor-mediated mechanisms (whether activation dependent or independent) may contribute to AMPA receptor internalization in response to synaptic release of glutamate, because synaptic activity (induced by picrotoxin) can stimulate AMPA receptor endocytosis in an NMDA receptor-independent manner. However, it is unclear to what extent the AMPA receptor endocytosis triggered by pharmacological treatment with AMPA is relevant to the physiological stimulation that occurs in synapses. Surprisingly, APV potentiated AMPA receptor internalization in response to picrotoxin, AMPA and CNQX, suggesting that the degree of AMPA receptor internalization is kept in check by synaptic NMDA receptor activity. Bath application of NMDA, however, accelerates AMPA receptor endocytosis (J.W.L. and M.S., unpublished observations). The finding that NMDA receptors can affect AMPA receptor internalization in opposing directions is not surprising given their critical involvement in both LTD and LTP.

Dephosphorylation of AMPA receptors is correlated with LTD[43–45], and both PP1 and calcineurin are implicated in LTD mechanisms[46]. LTD and insulin-induced synaptic depression depend on postsynaptic endocytosis[3,7] and are mutually occlusive[3], implying some shared mechanisms. We find that calcineurin and PP1 are also involved in insulin-stimulated AMPA receptor endocytosis. Our pharmacological data suggest that PP1 and calcineurin may be components of a common mechanism for AMPA receptor internalization that is shared in part by homosynaptic LTD and insulin-mediated synaptic depression. In apparent contrast to our results, Beattie *et al.*[47] in this issue found that calcineurin was required for AMPA-induced AMPA receptor internalization. Their experimental protocol may favor measurement of the activation-dependent mode of AMPA-stimulated internalization (involving calcium influx and hence calcineurin), whereas ours favored the ligand-dependent mode (calcium and calcineurin independent). Differences in culture density and drug treatment protocols could also contribute to other quantitative differences between the two studies.

Determinants for AMPA receptor internalization

The last 15 amino acids of GluR2 are required for insulin- but not AMPA- or DNQX-induced internalization in HEK cells. Within this region of GluR2 are three tyrosine residues (Y869, Y873 and Y876), mutations of which also eliminate insulin-induced GluR2 endocytosis (J. G. Mielke *et al.*, *Soc. Neurosci. Abstr.*, 425.11, 2000). Tyrosine is a critical component of Y-X-X-Φ and N-P-X-Y sequence motifs that are implicated in endocytosis. These motifs require tyrosine to be in the dephosphosphorylated state to bind to components of the clathrin coat such as μ-adaptin[48]. Although Y869, Y873 and Y876 do not

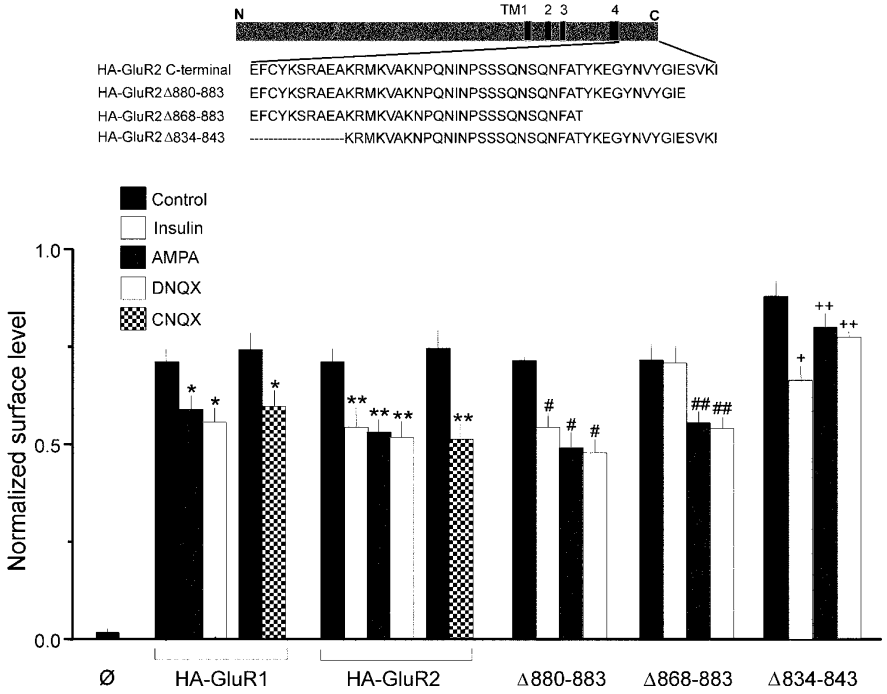

Fig. 7. Differential subunit and sequence requirements for AMPA- and insulin-induced AMPA receptor endocytosis. HA-tagged GluR1, GluR2 and cytoplasmic domain mutants of GluR2 (top, diagram) were expressed in HEK293 cells. The amount of pre-labeled surface receptor remaining at the cell surface at 30 min was measured by colorimetric cell-ELISA in the presence of vehicle control, 0.5 μM insulin, 100 μM AMPA, 30 μM DNQX or 30 μM CNQX, and expressed as a fraction of total surface receptor at $t = 0$. Untransfected cells (fl) showed negligible surface staining. Separate controls are shown for CNQX, as these experiments were performed separately. Internalization of HA-GluR1 in HEK cells is not stimulated by insulin[3]. * $p < 0.005$ compared with HA-GluR1 control; ** $p < 0.001$ compared with HA-GluR2 control; # $p < 0.001$ compared with Δ880–883 control; ## $p < 0.001$ compared with Δ868–883 control; + $p < 0.001$ compared with Δ834–843 control; ++ $p < 0.01$ compared with Δ834–843 control.

fall within sequences that conform to Y-X-X-Φ or N-P-X-Y internalization motifs, it is possible that they interact with the endocytotic machinery in unrecognized ways. It will be interesting to investigate whether these tyrosine residues can be phosphorylated and dephosphorylated to affect specific protein interactions of the GluR2 tail.

AMPA and CNQX/DNQX stimulate the endocytosis of GluR1, a subunit that is unresponsive to insulin[3]. Because both GluR1 and GluR2 are sensitive to ligand-induced internalization, the determinants of this effect likely lie within an intracellular region conserved between these subunits. Indeed, deletion of a membrane proximal segment of the GluR2 C-terminal tail that is highly conserved among GluR1–4 (Δ834–843, EFCYKSRAEA) inhibited AMPA/DNQX-stimulated GluR2 internalization. Deletion of this membrane-proximal segment also reduced constitutive internalization of GluR2 in HEK cells, suggesting that constitutive and ligand-dependent endocytosis have common molecular requirements.

Protein interactions involving the C-terminal tails of GluR subunits may regulate not only the endocytosis of surface receptors but also the sorting of AMPA receptors following internalization. Disruption of the binding of β2-adrenergic receptor to its PDZ protein partner EBP50/NHERF results in degradation of the receptor after endocytosis[49]. By analogy, interactions of GluR2 with PDZ-proteins GRIP or PICK1, perhaps regulated by phosphorylation[28], could govern AMPA receptor sorting into recycling or degradative pathways. Thus, an important next step will be to understand the dynamics of GluR-mediated protein interactions during AMPA receptor endocytosis and intracellular sorting.

Methods

Hippocampal cultures. Hippocampal cultures were prepared using a modified published protocol[50]. Coverslips were coated overnight in 250 μg/ml poly-D-lysine and 25 μg/ml laminin. Hippocampi from E19 Sprague-Dawley rats were trypsinized for 15 min. Dissociated neurons were plated in Neurobasal medium supplemented with B27, 0.5 μM glutamine and 12.5 μM glutamate in 12-well plates at 75000 per well for medium-density cultures and 600,000 per well for high-density cultures. At 4 days *in vitro* and every 7 days thereafter, cultures were fed by replacing half the medium with feeding medium (Neurobasal medium with B27 and 0.5 μM glutamine).

Fluorescence internalization assay. Live hippocampal neurons at 15–18 days *in vitro* were labeled for 10 min at 37°C with an antibody directed against the extracellular region of either GluR1 (Oncogene Research Products, Cambridge, Massachusetts) or GluR2 (Chemicon International, Temecula, California). After washing in PBS, 1 mM MgCl and 0.1 mM CaCl (PBS + MC), neurons were incubated at 37°C in conditioned growth medium containing pharmacological agents. Neurons were fixed for 5 min at room temperature in 4% paraformaldehyde/4% sucrose without permeabilization, and stained with FITC-conjugated secondary antibodies for 1 h at room temperature, to visualize pre-labeled surface receptors. Neurons were then permeabilized for 1 min in 100% methanol at –20°C and stained with Cy3-conjugated secondary antibodies for 1 h at room temperature, to visualize pre-labeled internalized receptors. In 'post-labeling' experiments, neurons were first treated for 20 min with either AMPA or insulin, after which they were labeled with extracellular GluR1 antibody for 10 min at 37°C and then allowed to undergo endocytosis for an additional 10 min in the continued presence of either AMPA or insulin. Fluorescence images were acquired using a Photometrics CCD camera (Princeton Instruments, Trenton, New Jersey) and quantified with Metamorph software (Universal Imaging Corporation, West Chester, Pennsylvania). Red fluorescence intensities indicative of internalization were divided by total (red + green) fluorescence intensities to control for cell density. Units of internalization were measured as red/total fluorescence normalized to untreated controls.

Surface biotinylation assay. Live hippocampal neurons were labeled for 2 min at 37°C with EZ-link NHS-SS-biotin (300 μg/ml, Pierce, Rockford, Illinois) to biotinylate surface proteins. After washing in Tris-buffered saline, neurons were incubated in medium alone or in medium containing 100 μM AMPA for various times. Trafficking was halted by rapid cooling to 4°C. Biotinylated proteins remaining on the cell surface were stripped of biotin by the non-permeant reducing agent glutathione (150 mM glutathione, 150 mM NaCl, pH 8.75). Glutathione was subsequently neutralized by 50 mM iodoacetamide in PBS + MC. Cells were lysed in extraction buffer (50 mM Tris, pH 7.4, 150 mM NaCl, 1 mM EDTA, 1% SDS) by boiling for 5 min. After centrifugation at 16000 *g*, supernatants containing equal amounts of total protein were incubated with streptavidin beads to capture biotinylated proteins. After washing in extraction buffer, biotinylated proteins were eluted from streptavidin beads by boiling in sample buffer, separated by SDS-PAGE and immunoblotted using antibodies against GluR1 (1:2000), TfR (1:250, Zymed Laboratories, San Francisco, California) and NR1 (1 μg/ml, PharMingen, San Diego, California). In post-labeling experiments, neurons were biotinylated for 2 min at 37°C, as described above, at 20 min after onset of AMPA or insulin treatment. Following biotinylation, neurons were allowed to undergo endocytosis for an additional 10 min in the continued presence of either AMPA or insulin. Immunoblots were processed by standard chemiluminescence protocol. Bands were digitized and quantified using a digital electrophoresis documentation and analysis system (Kodak, Rochester, New York). All band intensities were normalized to the band intensity of a biotinylated but unstripped sample (not treated with glutathione), which represented total surface protein at the time of biotinylation.

Dominant negative dynamin and AMPA receptor internalization. Wild-type and dominant negative (K44A) dynamin I cDNAs were used. Hippocampal neurons (15 days *in vitro*) were transfected with HA-tagged wild-type and K44A dynamin in GW1 expression vector using calcium phosphate. After 48 h, the immunofluorescence internalization assay was used to detect AMPA receptor internalization, but with the following modifications. After formaldehyde fixation, labeled surface receptors were blocked by 'cold' secondary antibody. Neurons were then permeabilized for 1 min in 100% methanol at –20°C and incubated overnight at 4°C in anti-HA antibody. The following day, neurons were labeled with FITC-conjugated secondary antibodies against the HA antibody and Cy3-conjugated secondary antibodies against internalized GluR1 antibody.

Colocalization of internalized AMPA receptors with endosomal markers. The immunofluorescence internalization assay was carried out to the point of formaldehyde fixation, and labeled surface receptors were blocked by excess 'cold' secondary antibody. Neurons were then permeabilized for 1 min in 100% methanol at –20°C and incubated overnight at 4°C in primary antibodies directed against EEA1 (1:250, Transduction Laboratories, Lexington, Kentucky), TfR (1:500), syntaxin 13 (1:1000) or Lamp1 (1:250, Stressgen Biotechnologies Corporation, Victoria, British Columbia, Canada). The following day, neurons were labeled with Cy3-conjugated secondary antibodies directed against internalized AMPA receptor antibodies and FITC-conjugated secondary antibodies directed against membrane compartment marker antibodies.

Cell ELISA assay. Cell ELISA 'colorimetric' assays were done using a protocol described previously[3]. HEK293 cells were transfected by the calcium phosphate method and replated 24 h later into 12-well plates. Surface GluR subunits (HA-tagged) were pre-labeled by incubating live cells at 4°C with 10 μg/ml monoclonal anti-HA antibody for 1 h. Cells were then returned to 37°C for 30 min in the presence of drug, and then fixed for 5 min in 2% paraformaldehyde without permeabilization. After washing, cells were sequentially incubated for 1 h at room temperature with horseradish peroxidase-conjugated secondary antibody (1:800; Amersham Pharmacia Biotech, Piscataway, New Jersey) and for 2 min with chromagenic substrate (OPD; Sigma, St. Louis, Missouri). Reactions were stopped with 0.2 volume 3 N HCl, and the optical density of 1 ml of supernatant was read on a spectrophotometer at 492 nm. Surface expression was described as a fraction of that measured on cells not subjected to the 30 minute incubation at 37°C.

ACKNOWLEDGEMENTS

We thank R.B. Vallee (Worcester Institute, Shrewsbury, Massachusetts) for dynamin I cDNAs, R. Scheller and R. Prekeris (Stanford University School of Medicine, Stanford, California) for syntaxin 13 antibodies, and R. Huganir (Johns Hopkins University, Baltimore, Maryland) for GluR1 antibodies. M.S. is Assistant Investigator of the Howard Hughes Medical Institute. Y.T.W. is a Research Scholar of the Heart and Stroke Foundation of Canada. Supported by grants from US National Institute of Health (NS35050) to M.S. and Heart and Stroke Foundation of Ontario (NA-3762), the Medical Research Council of Canada, and the EJLB Foundation to Y.T.W. S.H.L. was supported in part by a postdoctoral fellowship from KOSEF.

RECEIVED 29 SEPTEMBER; ACCEPTED 26 OCTOBER 2000

1. Dingledine, R., Borges, K., Bowie, D. & Traynelis, S. F. The glutamate receptor ion channels. *Pharmacol. Rev.* **51**, 7–61 (1999).
2. Turrigiano, G. G. AMPA receptors unbound: membrane cycling and synaptic plasticity. *Neuron* **26**, 5–8 (2000).
3. Man, Y. H. *et al.* Regulation of AMPA receptor-mediated synaptic transmission by clathrin-dependent receptor internalization. *Neuron* **25**, 649–662 (2000).
4. Wang, Y. T. & Linden, D. J. Expression of cerebellar long-term depression requires postsynaptic clathrin-mediated endocytosis. *Neuron* **25**, 635–647 (2000).
5. Hayashi, Y. *et al.* Driving AMPA receptors into synapses by LTP and CaMKII: requirement for GluR1 and PDZ domain interaction. *Science* **287**, 2262–2267 (2000).
6. Carroll, R. C., Lissin, D. V., von Zastrow, M., Nicoll, R. A. & Malenka, R. C. Rapid redistribution of glutamate receptors contributes to long-term depression in hippocampal cultures. *Nat. Neurosci.* **2**, 454–460 (1999).
7. Lüscher, C. *et al.* Role of AMPA receptor cycling in synaptic transmission and plasticity. *Neuron* **24**, 649–658 (1999).
8. Shi, S. H. *et al.* Rapid spine delivery and redistribution of AMPA receptors after synaptic NMDA receptor activation. *Science* **284**, 1811–1816 (1999).
9. Lissin, D. V. *et al.* Activity differentially regulates the surface expression of synaptic AMPA and NMDA glutamate receptors. *Proc. Natl. Acad. Sci. USA* **95**, 7097–7102 (1998).
10. Liao, D., Zhang, X., O'Brien, R., Ehlers, M. D. & Huganir, R. L. Regulation of morphological postsynaptic silent synapses in developing hippocampal neurons. *Nat. Neurosci.* **2**, 37–43 (1999).
11. Mammen, A. L., Huganir, R. L. & O'Brien, R. J. Redistribution and stabilization of cell surface glutamate receptors during synapse formation. *J. Neurosci.* **17**, 7351–7358 (1997).
12. O'Brien, R. J. *et al.* The development of excitatory synapses in cultured spinal neurons. *J. Neurosci.* **17**, 7339–7350 (1997).
13. Turrigiano, G. G., Leslie, K. R., Desai, N. S., Rutherford, L. & Nelson, S. B. Activity-dependent scaling of quantal amplitude in neocortical neurons. *Nature* **391**, 892–896 (1998).
14. O'Brien, R. J. *et al.* Activity-dependent modulation of synaptic AMPA receptor accumulation. *Neuron* **21**, 1067–1078 (1998).
15. Carroll, R. C. *et al.* Dynamin-dependent endocytosis of ionotropic glutamate receptors. *Proc. Natl. Acad. Sci. USA* **96**, 14112–14117 (1999).
16. Lledo, P.-M., Zhang, X., Südhof, T. C., Malenka, R. C. & Nicoll, R. A. Postsynaptic membrane fusion and long-term potentiation. *Science* **279**, 399–403 (1998).
17. Noel, J. *et al.* Surface expression of AMPA receptors in hippocampal neurons is regulated by an NSF-dependent mechanism. *Neuron* **23**, 365–376 (1999).
18. Luthi, A. *et al.* Hippocampal LTD expression involves a pool of AMPARs regulated by the NSF-GluR2 interaction. *Neuron* **24**, 389–399 (1999).
19. Dong, H. *et al.* GRIP: a synaptic PDZ domain-containing protein that interacts with AMPA receptors. *Nature* **386**, 279–284 (1997).
20. Srivastava, S. *et al.* Novel anchorage of GluR2/3 to the postsynaptic density by the AMPA receptor-binding protein ABP. *Neuron* **21**, 581–591 (1998).
21. Xia, J., Zhang, X., Staudinger, J. & Huganir, R. L. Clustering of AMPA receptors by the synaptic PDZ domain-containing protein PICK1. *Neuron* **22**, 179–187 (1999).
22. Nishimune, A. *et al.* NSF binding to GluR2 regulates synaptic transmission. *Neuron* **21**, 87–97 (1998).
23. Osten, P. *et al.* The AMPA receptor GluR2 C terminus can mediate a reversible, ATP-dependent interaction with NSF and alpha- and beta-SNAPs. *Neuron* **21**, 99–110 (1998).
24. Song, I. *et al.* Interaction of the N-ethylmaleimide-sensitive factor with AMPA receptors. *Neuron* **21**, 393–400 (1998).
25. Wyszynski, M. *et al.* Association of AMPA receptors with a subset of glutamate receptor-interacting protein in vivo. *J. Neurosci.* **19**, 6528–6537 (1999).
26. Leonard, A. S., Davare, M. A., Horne, M. C., Garner, C. C. & Hell, J. W. SAP97 is associated with the alpha-amino-3-hydroxy-5-methylisoxazole-4-propionic acid receptor GluR1 subunit. *J. Biol. Chem.* **273**, 19518–19524 (1998).
27. Li, P. *et al.* AMPA receptor–PDZ interactions in facilitation of spinal sensory synapses. *Nat. Neurosci.* **2**, 972–977 (1999).
28. Matsuda, S., Mikawa, S. & Hirai, H. Phosphorylation of serine-880 in GluR2 by protein kinase C prevents its C terminus from binding with glutamate receptor-interacting protein. *J. Neurochem.* **73**, 1765–1768 (1999).
29. Musaro, A., McCullagh, K. J., Naya, F. J., Olson, E. N. & Rosenthal, N. IGF-1 induces skeletal myocyte hypertrophy through calcineurin in association with GATA-2 and NF-ATc1. *Nature* **400**, 581–585 (1999).
30. Semsarian, C. *et al.* Skeletal muscle hypertrophy is mediated by a Ca^{2+}-dependent calcineurin signalling pathway. *Nature* **400**, 576–581 (1999).
31. Lai, M. M. *et al.* The calcineurin-dynamin 1 complex as a calcium sensor for synaptic vesicle endocytosis. *J. Biol. Chem.* **274**, 25963–25966 (1999).
32. Advani, R. J. *et al.* Seven novel mammalian SNARE proteins localize to distinct membrane compartments. *J. Biol. Chem.* **273**, 10317–10324 (1998).
33. Prekeris, R., Klumperman, J., Chen, Y. A. & Scheller, R. H. Syntaxin 13 mediates cycling of plasma membrane proteins via tubulovesicular recycling endosomes. *J. Cell. Biol.* **143**, 957–971 (1998).
34. Christoforidis, S., McBride, H. M., Burgoyne, R. D. & Zerial, M. The Rab5 effector EEA1 is a core component of endosome docking. *Nature* **397**, 621–625 (1999).
35. McBride, H. M. *et al.* Oligomeric complexes link Rab5 effectors with NSF and drive membrane fusion via interactions between EEA1 and syntaxin 13. *Cell* **98**, 377–386 (1999).
36. Gaullier, J. M., Ronning, E., Gillooly, D. J. & Stenmark, H. Interaction of the EEA1 FYVE finger with phosphatidylinositol 3- phosphate and early endosomes. Role of conserved residues. *J. Biol. Chem.* **275**, 24595–24600 (2000).
37. Simonsen, A. *et al.* EEA1 links PI(3)K function to Rab5 regulation of endosome fusion. *Nature* **394**, 494–498 (1998).
38. Yamashiro, D. J., Tycko, B., Fluss, S. R. & Maxfield, F. R. Segregation of transferrin to a mildly acidic (pH 6.5) para-Golgi compartment in the recycling pathway. *Cell* **37**, 789–800 (1984).
39. Mayor, S., Presley, J. F. & Maxfield, F. R. Sorting of membrane components from endosomes and subsequent recycling to the cell surface occurs by a bulk flow process. *J. Cell. Biol.* **121**, 1257–1269 (1993).
40. Mellman, I. Endocytosis and molecular sorting. *Annu. Rev. Cell. Dev. Biol.* **12**, 575–625 (1996).
41. Willins, D. L. *et al.* Clozapine and other 5-hydroxytryptamine-2A receptor antagonists alter the subcellular distribution of 5-hydroxytryptamine-2A receptors in vitro and in vivo. *Neuroscience* **91**, 599–606 (1999).
42. Merlin, L. & Wong, R. Synaptic modifications accompanying epileptogenesis in vitro: long-term depression of GABA-mediated inhibition. *Brain Res.* **627**, 330–340 (1993).
43. Kameyama, K., Lee, H. K., Bear, M. F. & Huganir, R. L. Involvement of a postsynaptic protein kinase A substrate in the expression of homosynaptic long-term depression. *Neuron* **21**, 1163–1175 (1998).
44. Lee, H. K., Kameyama, K., Huganir, R. L. & Bear, M. F. NMDA induces long-term synaptic depression and dephosphorylation of the GluR1 subunit of AMPA receptors in hippocampus. *Neuron* **21**, 1151–1162 (1998).
45. Lee, H.-K., Barbarosie, M., Kameyama, K., Bear, M. F. & Huganir, R. L. Regulation of distinct AMPA receptor phosphorylation sites during bidirectional synaptic plasticity. *Nature* **405**, 955–959 (2000).
46. Mulkey, R. M., Endo, S., Shenolikar, S. & Malenka, R. C. Involvement of a calcineurin/inhibitor-1 phosphatase cascade in hippocampal long-term depression. *Nature* **369**, 486–488 (1994).
47. Beattie, E. C. *et al.* Regulation of AMPA receptor endocytosis by a signaling mechanism shared with LTD. *Nat. Neurosci.* **3**, AAA–BBB (2000).
48. Kirchhausen, T., Bonifacino, J. S. & Riezman, H. Linking cargo to vesicle formation: receptor tail interactions with coat proteins. *Curr. Opin. Cell. Biol.* **9**, 488–495 (1997).
49. Cao, T. T., Deacon, H. W., Reczek, D., Bretscher, A. & von Zastrow, M. A kinase-regulated PDZ-domain interaction controls endocytic sorting of the beta2-adrenergic receptor. *Nature* **401**, 286–290 (1999).
50. Brewer, G. J., Torricelli, J. R., Evege, E. K. & Price, P. J. Optimized survival of hippocampal neurons in B27-supplemented Neurobasal, a new serum-free medium combination. *J. Neurosci. Res.* **35**, 567–576 (1993).